in Ref. 2.

[8]X. Zubarov, Usp. Fiz. Nauk 71, 71 (1960) [Soviet Phys. Usp. 3, 320 (1960)].

[9]This approximation does, however, place an upper limit on the distance into the metal electrode we can place the magnetic impurity (Einstein phonon in our second model), and still maintain the validity of our calculations using Eq. (2.22) or Eq. (3.6). An estimate of this distance z is easily obtained from Eqs. (2.11) and (2.26). The allowed values of the transverse energy $\epsilon_{\vec{k}\perp}$, are confined by the exponential tunneling matrix element to be $\sim \kappa/2b$, for which k varies by $(k_F/4b)\,\kappa/\epsilon_F$. This results in a variation of kA, in the cosine and sine factors in Eqs. (2.26) and (2.27), which becomes important when it is of order 1. From this we see that $|z_0+b|$ should be less than $2b$ in order to set $\vec{k}_\perp = 0$ everywhere but in the exponential.

[10]L. C. Davis, Phys. Rev. 187, 1177 (1969).

[11]L. Y. L. Shen and J. M. Rowell, Solid State Commun. 5, 189 (1967).

[12]E. T. Wolf and D. L. Losie, Solid State Commun. 7, 665 (1969).

[13]J. M. Rowell, W. L. McMillan, and W. L. Feldmann, Phys. Rev. 180, 658 (1969).

[14]R. C. Jacklevic and J. Lambe, Bull. Am. Phys. Soc. 14, 43 (1969).

[15]J. G. Adler, Phys. Letters 29A, 675 (1969).

[16]L. C. Davis and C. B. Duke, Phys. Rev. 184, 764 (1969).

Noninteracting Band Model for Dielectric Screening in Transition Metals: Application to Paramagnetic Nickel

Satya Prakash and S. K. Joshi

Physics Department, University of Roorkee, Roorkee, India

(Received 17 February 1970)

The static dielectric function is studied for a transition metal on the basis of a model band structure with noninteracting s and d bands. The free-electron approximation is used for electrons in the s band, while a simplified tight-binding scheme is used for the d electrons. Explicit expressions are obtained for the intraband and interband contributions to the dielectric function. The model is applied to calculate the static dielectric function for paramagnetic nickel for $(3d)^9\,(4s)^1$ and $(3d)^{9.4}\,(4s)^{0.6}$ configurations along the three principal symmetry directions [100], [110], and [111]. The contributions due to the intraband and interband transitions are compared: It is found that the major contribution to the dielectric function is due to the intraband transitions.

I. INTRODUCTION

The response of a many-electron system to an external perturbation can be discussed in terms of the frequency and wave-number–dependent dielectric function $\epsilon(\vec{q}, \omega)$.[1] Here $\vec{q}$ is the wave number and ω is the frequency. Nozières and Pines[2] and Ehrenreich and Cohen[3] deduced explicit expressions for the longitudinal component of the dielectric tensor within the random-phase approximation, and they did not consider the local field effects. Adler[4] deduced an integral equation for the generalized dielectric tensor, including local field effects, and discussed some limiting cases of the general expression. When we are dealing with a system of nearly free electrons, the complex expression for the dielectric function reduces to a simple form. There have been attempts at evaluation of the dielectric function for semiconductors,[5-7] but because of the difficulties introduced by the presence of d electrons, not much work has been done on the problem of dielectric screening in the transition metals. Recently, Hayashi and Shimizu[8] studied the dielectric screening in a transition metal. They considered two models, first a single-band model for d electrons and then a two-band model for s- and d-band electrons. They did not consider explicitely the contribution from the interband transitions.

In this paper, an explicit expression for the longitudinal component of the static dielectric tensor for a transition metal is deduced. The formalism, presented in Sec. II, is applied to the specific case of paramagnetic nickel in Sec. III. The results are discussed in Sec. IV.

II. THEORY

The general expression for the longitudinal static dielectric matrix in the random-phase approximation is[9]

$$\epsilon(\vec{q}+\vec{G},\ \vec{q}+\vec{G}') = \delta_{GG'} - \frac{4\pi e^2}{N\Omega_0(\vec{q}+\vec{G})^2} \sum_k \sum_H \sum_{lm} \sum_{l'm'} \{[n_{lm}(\vec{k}) - n_{l'm'}(\vec{k}+\vec{q}+\vec{H})]/[E_{lm}(\vec{k}) - E_{l'm'}(\vec{k}+\vec{q}+\vec{H})]\}$$
$$\times \langle \psi_{lm}(\vec{k}) | \exp[-i(\vec{q}+\vec{G})\cdot\vec{r}\,] | \psi_{l'm'}(\vec{k}+\vec{q}+\vec{H}) \rangle \langle \psi_{l'm'}(\vec{k}+\vec{q}+\vec{H}) | \exp[i(\vec{q}+\vec{G}')\cdot\vec{r}\,] | \psi_{lm}(\vec{k}) \rangle . \quad (1)$$

Here N is the number of unit cells in the crystal; Ω_0 is the volume of the unit cell; $\vec{G}, \vec{G}'$, and $\vec{H}$ are the reciprocal-lattice vectors; the orbital quantum number l and magnetic quantum number m act as the band indices; $E_{lm}(\vec{k})$ and $\psi_{lm}(\vec{k})$ are the eigenvalues and eigenfunctions, respectively, corresponding to the state specified by the wave vector $\vec{k}$; $n_{lm}(\vec{k})$ is the Fermi occupation-probability function for the state $\vec{k}$ for the band specified by the indices lm; $\vec{q}$ is the phonon wave vector; and e is the electronic charge. The summation on $\vec{k}$ is over all the occupied electronic states. We rewrite Eq. (1) in the form

$$\epsilon(\vec{q}+\vec{G}\cdot\vec{q}+\vec{G}') \equiv \delta_{GG'} - F(\vec{q}+\vec{G},\vec{q}+\vec{G}')|\vec{q}+\vec{G}|^{-2}, \quad (2)$$

where F has the obvious explanation. If we use the orthogonality condition

$$\sum_{G''} \epsilon(\vec{q}+\vec{G},\vec{q}+\vec{G}'')\,\epsilon^{-1}(\vec{q}+\vec{G}'',\vec{q}+\vec{G}') = \delta_{GG'}, \quad (3)$$

we obtain

$$\epsilon^{-1}(\vec{q}+\vec{G},\vec{q}+\vec{G}') = \delta_{GG'} + \sum_{G''} F(\vec{q}+\vec{G},\vec{q}+\vec{G}'')$$
$$\times \epsilon^{-1}(\vec{q}+\vec{G}'',\vec{q}+\vec{G}')|\vec{q}+\vec{G}|^{-2}. \quad (4)$$

This is the general expression for the longitudinal inverse dielectric matrix obtained by Adler[4] and Wiser.[10]

In order to render the dielectric matrix (1) tractable to calculation, a model band structure is assumed for the transition metal. Let z_s and z_d be the number of electrons per atom in the s and d bands, respectively. The different d subbands are characterized by the values of m. Because of the presence of the perturbing field with wave vector $\vec{q}$, the electrons themselves undergo the intraband and interband transitions and redistribute themselves. In this model, the dielectric matrix of Eq. (1) can be written in the form

$$\epsilon(\vec{q}+\vec{G},\vec{q}+\vec{G}') = \delta_{GG'} - \epsilon_{ss}(\vec{q}+\vec{G},\vec{q}+\vec{G}') - \epsilon_{dd}(\vec{q}+\vec{G},\vec{q}+\vec{G}') - \epsilon_{ds}(\vec{q}+\vec{G},\vec{q}+\vec{G}') - \epsilon_{sd}(\vec{q}+\vec{G},\vec{q}+\vec{G}'), \quad (5)$$

where $\epsilon_{ss}(\vec{q}+\vec{G},\vec{q}+\vec{G}') = V(\vec{q}+\vec{G}) \sum_k \sum_H \{[n_s(\vec{k}) - n_s(\vec{k}+\vec{q}+\vec{H})]/[E_s(\vec{k}) - E_s(\vec{k}+\vec{q}+\vec{H})]\}$
$$\times \langle \psi_s(\vec{k}) | \exp[-i(\vec{q}+\vec{G})\cdot\vec{r}\,] | \psi_s(\vec{k}+\vec{q}+\vec{H}) \rangle \langle \psi_s(\vec{k}+\vec{q}+\vec{H}) | \exp[i(\vec{q}+\vec{G}')\cdot\vec{r}\,] | \psi_s(\vec{k}) \rangle , \quad (6)$$

$$\epsilon_{dd}(\vec{q}+\vec{G},\vec{q}+\vec{G}') = V(\vec{q}+\vec{G}) \sum_k \sum_H \sum_{m,m'} \{[n_{dm}(\vec{k}) - n_{dm'}(\vec{k}+\vec{q}+\vec{H})]/[E_{dm}(\vec{k}) - E_{dm'}(\vec{k}+\vec{q}+\vec{H})]\}$$
$$\times \langle \psi_{dm}(\vec{k}) | \exp[-i(\vec{q}+\vec{G})\cdot\vec{r}\,] | \psi_{dm'}(\vec{k}+\vec{q}+\vec{H}) \rangle \langle \psi_{dm'}(\vec{k}+\vec{q}+\vec{H}) | \exp[i(\vec{q}+\vec{G}')\cdot\vec{r}\,] | \psi_{dm}(\vec{k}) \rangle , \quad (7)$$

$$\epsilon_{ds}(\vec{q}+\vec{G},\vec{q}+\vec{G}') = V(\vec{q}+\vec{G}) \sum_k \sum_H \sum_m \{[n_{dm}(\vec{k}) - n_s(\vec{k}+\vec{q}+\vec{H})]/[E_{dm}(\vec{k}) - E_s(\vec{k}+\vec{q}+\vec{H})]\}$$
$$\times \langle \psi_{dm}(\vec{k}) | \exp[-i(\vec{q}+\vec{G})\cdot\vec{r}\,] | \psi_s(\vec{k}+\vec{q}+\vec{H}) \rangle \langle \psi_s(\vec{k}+\vec{q}+\vec{H}) | \exp[i(\vec{q}+\vec{G}')\cdot\vec{r}\,] | \psi_{dm}(\vec{k}) \rangle . \quad (8)$$

Here $V(\vec{q}) = 4\pi e^2/N\Omega_0 q^2$.

The expression for ϵ_{sd} is obtained by interchanging the subscripts s and dm in (8).

A. Evaluation of $\epsilon_{ss}(\vec{q}+\vec{G},\vec{q}+\vec{G}')$

We have used the plane-wave approximation for the s band,

$$\psi_s(\vec{k}) = (N\Omega_0)^{-1/2} \exp(i\vec{k}\cdot\vec{r}) \quad (9)$$

and $$E_s(\vec{k}) = E_s^0 + \hbar^2k^2/2m_s, \quad (10)$$

where m_s is the effective mass for the s band and E_s^0 is the energy at $\vec{k}=0$ in the s band. With these approximations, (6) simplifies to the familiar expression

$$\epsilon_{ss}(\vec{p}) = -\frac{2m_s k_{Fs} e^2}{\pi\hbar^2 p^2}\left(1 + \frac{4k_{Fs}^2 - p^2}{4k_{Fs}p} \ln\left|\frac{2k_{Fs}+p}{2k_{Fs}-p}\right|\right). \quad (11)$$

Here the Fermi sphere for s electrons has the radius

$$k_{Fs} = (3z_s\pi^2/\Omega_0)^{1/3} \text{ and } \vec{p} = \vec{q} + \vec{H}.$$

B. Evaluation of $\epsilon_{dd}(\vec{q}+\vec{G}, \vec{q}+\vec{G}')$

We use the simple tight-binding functions for the d electrons

$$\psi_{dm}(\vec{k}) = (N)^{-1/2} \sum_L \exp(i\vec{k}\cdot\vec{L})\,\phi_{dm}(\vec{r}-\vec{L}), \quad (12)$$

where $\vec{L}$ is the lattice vector. We write the d-electron energies in various d subbands in the effective-mass approximation

$$E_{dm}(\vec{k}) = E^0_{dm} + \hbar^2k^2/2m_{dm}, \quad (13)$$

where m_{dm} is the effective mass for the mth d subband and E^0_{dm} is the value of $E_{dm}(\vec{k})$ for $\vec{k}=0$. If we write $\vec{p}' = \vec{q}+\vec{G}$ and use (12), we can write the matrix element occurring in Eq. (7) in the form

$$\int_{N\Omega_0} \psi^*_{dm}(\vec{k}) \exp(-i\vec{p}'\cdot\vec{r})\psi_{dm'}(\vec{k}+\vec{p})\,d\vec{r} = \delta_{pp'} \int \phi^*_{dm}(\vec{r}) \exp(-i\vec{p}'\cdot\vec{r})\phi_{dm'}(\vec{r})\,d\vec{r}$$

$$+ (1/N)\sum_L \sum_{L'}{}' \exp[-i\vec{k}\cdot(\vec{L}-\vec{L}')] \exp[i(\vec{p}\cdot\vec{L}'-\vec{p}'\cdot\vec{L})] \int \phi^*_{dm}(\vec{r}) \exp(-i\vec{p}'\cdot\vec{r})\,\phi_{dm'}(\vec{r}+\vec{L}-\vec{L}')\,d\vec{r}. \quad (14)$$

The prime on the summation indicates that the term $L = L'$ is excluded. We neglect the multicenter integrals, and the above matrix element reduces to

$$\delta_{pp'}\Delta_{dm,dm'}(\vec{p}'), \quad (15)$$

where $\Delta_{dm,dm'}(\vec{p}')$ is the integral in the first term of Eq. (14). The other matrix element occurring in (7) is given by the complex conjugate of (15). Because of the δ functions present in the matrix elements, the dielectric matrix reduces to the diagonal form, and we get

$$\epsilon_{dd}(\vec{p}) = 2V(\vec{p}) \sum_m \sum_{m'} \Delta_{dm,dm'}(\vec{p})\,\Delta^*_{dm,dm'}(p) \times \sum_k \{n_{dm}(\vec{k})/[E_{dm}(\vec{k}) - E_{dm'}(\vec{k}+\vec{q}+H)]\}. \quad (16)$$

1. *Case* (i): $m = m'$

This corresponds to intraband transitions in a subband. In this case, we find that

$$\epsilon_{dd}(\vec{p}) = -\frac{2e^2}{p^2\pi\hbar^2} \sum_m m_{dm}k_{Fdm} |\Delta_{dm,dm'}(\vec{p})|^2 \times \left(1 + \frac{4k_{Fdm}-p^2}{4k_{Fdm}p} \ln\left|\frac{2k_{Fdm}+p}{2k_{Fdm}-p}\right|\right).$$

Here k_{Fdm} is a wave vector for the highest occupied state in the subband dm and is given by $k_{Fdm} = (3\pi^2 z_{dm}/\Omega_0)^{1/3}$.

2. *Case* (ii): $m \neq m'$

Here we have to consider the transitions from one subband to another subband. We rewrite Eq. (16) in the form

$$\epsilon_{dd}(\vec{p}) = 2V(\vec{p}) \sum_m \sum_{m'}{}' \Delta_{dm,dm'}(\vec{p})\,\Delta^*_{dm,dm'}(\vec{p})\,I_k, \quad (18)$$

where

$$I_k = \frac{z_{dm}N}{\frac{4}{3}\pi k^3_{Fdm}} \times \int_0^{k_{Fdm}} \frac{d\vec{k}}{\hbar^2k^2/2m_{dm} - [(\hbar^2|\vec{k}+\vec{p}|^2)/2m_{dm'}]}, \quad (19)$$

and the prime on $\sum$ indicates that the term $m = m'$ is excluded. Evaluation of the above integrals yields[11]

$$\epsilon_{dd}(\vec{p}) = \sum_m \sum_{m'}{}' \Delta_{dm,dm'}(\vec{p})\,\Delta^*_{dm,dm'}(\vec{p}) \frac{8e^2m_{dm'}}{p^2\pi\hbar^2}(I_p + I_q), \quad (20)$$

where $$I_p = \frac{k_{Fdm}}{\xi} - \left[\frac{k^2_{Fdm}}{4p} - \frac{p}{4\xi}\left(1+\frac{2}{\xi}\right)\right] \times \ln\left|\frac{2k_{Fdm}p - k^2_{Fdm}\xi + p^2}{2k_{Fdm}p + k^2_{Fdm}\xi - p^2}\right|, \quad (21)$$

and

$$I_q = \frac{p^2}{\xi}\left(1+\frac{1}{\xi}\right)(-\lambda)^{-1/2}\left(\ln\left|\frac{-2p+2\xi k_{Fdm} - (-\lambda)^{1/2}}{-2p+2\xi k_{Fdm} + (-\lambda)^{1/2}}\right| + \ln\left|\frac{2p+2\xi k_{Fdm} - (-\lambda)^{1/2}}{2p+2\xi k_{Fdm} + (-\lambda)^{1/2}}\right|\right) \text{ if } \lambda < 0 \quad (22)$$

$$= (p^2/\xi)[1+(1/\xi)]\,2(\lambda)^{-1/2}[\tan^{-1}(-2p+2\xi k_{Fdm})(\lambda)^{-1/2} + \tan^{-1}(2p+2\xi k_{Fdm})(\lambda)^{-1/2}] \text{ if } \lambda > 0. \quad (23)$$

Here $$\lambda = -4p^2(\xi+1) \quad (24)$$

and $$\xi = (m_{dm'}/m_{dm}) - 1. \quad (25)$$

The analytical expressions for $\Delta_{dm,dm'}(p)$ are given in Appendix A.

C. Evaluation of $\epsilon_{ds}(\vec{q}+\vec{G}, \vec{q}+\vec{G}')$

We substitute for $\psi_s(\vec{k})$ and $\psi_{dm}(\vec{k})$ from (9) and

(12), respectively, in the matrix element occurring in (8) to obtain

$$\int_{n\Omega_0} \psi^*_{dm}(\vec{k}) \exp(-i\vec{p}' \cdot \vec{r}) \psi_s(\vec{k}+\vec{p})\, d\vec{r} = (\Omega_0)^{-1/2} \delta_{pp'} \int_{n\Omega_0} \phi^*_{dm}(\vec{r}) \exp(i\vec{k} \cdot \vec{r})\, d\vec{r} . \quad (26)$$

The other matrix element in (8) is the complex conjugate of (26). Combining (26) and (8), we get

$$\epsilon_{ds}(\vec{p}', \vec{p}'') = V(\vec{p}') \sum_k \sum_H \sum_m \frac{n_{dm}(\vec{k}) - n_s(\vec{k}+\vec{q}+\vec{H})}{E_{dm}(\vec{k}) - E_s(\vec{k}+\vec{q}+\vec{H})} \times \delta_{pp'} \delta_{p'p''} (1/\Omega_0) \int_{n\Omega_0} \phi^*_{dm}(\vec{r}) \exp(i\vec{k} \cdot \vec{r})\, d\vec{r} \times \int_{n\Omega_0} \phi_{dm}(\vec{r}) \exp(-i\vec{k} \cdot \vec{r})\, d\vec{r} . \quad (27)$$

The presence of the δ functions renders $\epsilon_{ds}(\vec{p}', \vec{p}'')$ diagonal. The transitions to be considered here are from the d band to the s band. Therefore, the sum over the initial states $\vec{k}$ is to be carried out over all the occupied states in the subband dm. The state $\vec{k}+\vec{q}+\vec{H}$ in the s band should be unoccupied for the transitions to take place. Therefore,

$$\epsilon_{ds}(\vec{p}) = \frac{V(\vec{p})}{\Omega_0} \sum_m \sum_k \frac{n_{dm}(\vec{k})}{E_{dm}(\vec{k}) - E_s(\vec{k}+\vec{p})} \int_{n\Omega_0} \phi^*_{dm}(\vec{r}) \times \exp(i\vec{k} \cdot \vec{r})\, d\vec{r} \int_{n\Omega_0} \phi_{dm}(\vec{r}) \exp(-i\vec{k} \cdot \vec{r})\, d\vec{r} . \quad (28)$$

These integrals can be simplified (see Appendix A) to give

$$\epsilon_{ds}(\vec{p}) = \frac{V(\vec{p})}{\Omega_0} \sum_m \sum_k \frac{(4\pi)^2 [F_2(k)]^2}{E_{dm}(\vec{k}) - E_s(\vec{k}+\vec{p})} \times Y_2^m{}^*(\theta_k, \phi_k)\, Y_2^m(\theta_k, \phi_k) . \quad (29)$$

Here θ_k and ϕ_k are the polar angles of vector $\vec{k}$ and

$$F_2(k) = \int_0^\infty j_2(kr)\, R_{3d}(r)\, r^2\, dr . \quad (30)$$

$j_n(kr)$ are the spherical Bessel functions and $R_{3d}(r)$ is the $3d$ radial wave function. Using (A8) in (30), we get

$$F_2(k) = 48\, k^2 \sum_{i=1}^{4} \frac{a_i\, \alpha_i}{(\alpha_i^2 + k^2)^4} . \quad (31)$$

The symbols are explained in Appendix A. Using the approximations (10) and (13) for $E_s(\vec{k}+\vec{p})$ and $E_{dm}(\vec{k})$, respectively, and replacing the sum over k by integration, (29) yields

$$\epsilon_{ds}(\vec{p}) = \frac{4\pi e^2}{\Omega_0 p^2} (4\pi)^2 \frac{2m_s}{\hbar^2} \frac{2}{8\pi^3} \sum_m \int_0^{k_{Fdm}} [F_2(k)]^2 k^2\, dk \times \int_0^{\pi} \int_0^{2\pi} \frac{Y_2^m{}^*(\theta_k, \phi_k)\, Y_2^m(\theta_k, \phi_k)}{a - b\cos\theta_{kp}}\, d\Omega_k . \quad (32)$$

Here $k_{Fdm} = (3\pi^2 z_{dm}/\Omega_0)^{1/3}$,

$$a = k^2[(m_s/m_{dm}) - 1] - p^2 , \quad (33)$$

and $b = 2kp$.

z_{dm} is the number of electrons per atom in the subband dm, θ_{kp} is the angle between the vectors $\vec{k}$ and $\vec{p}$, and $d\Omega_k$ is the solid angle. The evaluation of the angular integration is tedious and is given in Appendix B. The final expression for $\epsilon_{ds}(\vec{p})$ is

$$\epsilon_{ds}(\vec{p}) = \frac{32e^2}{\Omega_0 p^2} \frac{m_s}{\hbar^2} \sum_m (-1)^m \left\{ \int_0^{k_{Fdm}} [F_2(k)]^2 k^2\, dk \right\} \times [D^2_{0m} D^2_{0-m} I_0 + (D^2_{1m} D^2_{-1-m} + D^2_{-1m} D^2_{1-m}) I_1 + (D^2_{2m} D^2_{-2-m} + D^2_{-2m} D^2_{2-m}) I_2] . \quad (34)$$

$D^l_{m',m}$ are the elements of rotation matrices[12] with argument $(-\gamma, -\beta, -\alpha)$, where α, β, γ are the Euler angles. I_0, I_1, and I_2 are defined by Eq. (B8). We find

$$I_0 = \tfrac{5}{4}(\tfrac{1}{2} I_{n0} - 3I_{n2} + \tfrac{9}{2} I_{n4}),$$
$$I_1 = \tfrac{15}{4}(-I_{n2} + I_{n4}), \quad (35)$$
$$I_2 = \tfrac{15}{8}(\tfrac{1}{2} I_{n0} - I_{n2} + \tfrac{1}{2} I_{n4}),$$

where

$$I_{n0} = -\frac{1}{b} \ln\left|\frac{b-a}{b+a}\right| ,$$
$$I_{n2} = -\frac{1}{b}\left(\frac{2a}{b} + \frac{a^2}{b^2} \ln\left|\frac{b-a}{b+a}\right|\right) , \quad (36)$$
$$I_{n4} = -\frac{1}{b}\left(\frac{2a}{3b} + \frac{2a^3}{b^3} + \frac{a^4}{b^4} \ln\left|\frac{b-a}{b+a}\right|\right) .$$

D. Evaluation of $\epsilon_{sd}(\vec{q}+\vec{G}, \vec{q}+\vec{G}')$

Here we proceed in a manner analogous to that used for deriving the expression for $\epsilon_{ds}(\vec{p})$. However, we have to consider the transitions from the s band to the d subbands. We find

$$\epsilon_{sd}(\vec{p}) = \frac{V(\vec{p})}{\Omega_0} \sum_k \sum_m \frac{(4\pi)^2 [F_2(|\vec{k}+\vec{p}|)]^2}{E_s(\vec{k}) - E_{dm}(\vec{k}+\vec{p})} \times Y_2^m(\theta_{k+p}, \phi_{k+p})\, Y_2^m{}^*(\theta_{k+p}, \phi_{k+p}) , \quad (37)$$

where θ_{k+p}, ϕ_{k+p} are the polar angles of the vector $\vec{k}+\vec{p}$. The summation over $\vec{k}$ is over all the occupied states in the s band. Using Eqs. (10) and (13) for $E_s(\vec{k})$ and $E_{dm}(\vec{k}+\vec{p})$, respectively, we obtain

$$\epsilon_{sd}(\vec{p}) = \frac{32e^2}{\Omega_0 p^2 \hbar^2} \sum_m m_{dm} \int_0^{k_{Fs}} k^2\, dk \int_0^{\pi} \int_0^{2\pi} \frac{[F_2(|\vec{k}+\vec{p}|)]^2\, Y_2^m(\theta_{k+p}, \phi_{k+p})\, Y_2^{m*}(\theta_{k+p}, \phi_{k+p})\, d\Omega_k}{a' - b\cos\theta_{kp}}\ , \tag{38}$$

where $a' = k^2(m_{dm}/m_s - 1) - p^2$. (39)

The angular part of the integral (38) is discussed in Appendix C. Using (C2), we can write

$$\epsilon_{sd}(\vec{p}) = \frac{32e^2}{\Omega_0 p^2 \hbar^2} \sum_m m_{dm}(-1)^m [D_{0m}^2 D_{0-m}^2 \int_0^{k_{Fs}} I_0' k^2\, dk + (D_{-1m}^2 D_{1-m}^2 + D_{1m}^2 D_{-1-m}^2) \int_0^{k_{Fs}} I_1' k^2\, dk + (D_{-2m}^2 D_{2-m}^2 + D_{2m}^2 D_{-2-m}^2) \int_0^{k_{Fs}} I_2' k^2\, dk]. \tag{40}$$

I_0', I_1', and I_2' are obtained with the help of (C3), (C4), and (30):

$$I_0' = \tfrac{5}{8}(48)^2 \sum_{i=1}^{4} \sum_{j=1}^{4} a_i a_j \alpha_i \alpha_j \times \int_{-1}^{+1} (2p^2 - k^2 + 3k^2t^2 + 4pkt)^2\, dt\, [S(t)]^{-1}, \tag{41}$$

with $S(t) = (\alpha_i^2 + k^2 + p^2 + 2kpt)^4 \times (\alpha_j^2 + k^2 + p^2 + 2kpt)^4 (a' - bt)$, (42)

$$I_1' = -\tfrac{15}{4}(48)^2 \sum_{i=1}^{4} \sum_{j=1}^{4} a_i a_j \alpha_i \alpha_j \times \int_{-1}^{+1} \frac{[(p+kt)^2(k^2+p^2+2kpt) - (p+kt)^4]\, dt}{S(t)}, \tag{43}$$

and $I_2' = \tfrac{15}{16}(48)^2 \sum_{i=1}^{4} \sum_{j=1}^{4} a_i a_j \alpha_i \alpha_j \int_{-1}^{+1} \frac{k^4(t^2-1)^2\, dt}{S(t)}$. (44)

The integrals in (42)–(44) can be evaluated by using the method of partial fractions for the two cases $i = j$ and $i \neq j$ separately. The final expressions are very lengthy and we do not give them here. In fact, the numerical integration proved to be more convenient for these equations.

E. Evaluation of ϵ_{ds} and ϵ_{sd} in Free-Electron Approximation

The expressions for ϵ_{ds} and ϵ_{sd} are quite complicated even when we use extremely simple forms for wave functions of s and d electrons. We therefore thought it interesting to evaluate ϵ_{ds} and ϵ_{sd} by adopting the free-electron approximation for electrons in the d band also. The electron energies are written by using the approximations (10) and (13). ϵ_{ds} is given by

$$\epsilon_{ds}(\vec{p}) = \frac{4m_s}{\pi a_0}\frac{1}{p^2} \sum_m \left\{ I_{dm} + \frac{p^2}{\eta}\left(1+\frac{1}{\eta}\right)(-\mu_1)^{-1/2} \left[\ln\left| \frac{2\eta k_{Fdm} - 2p - (-\mu_1)^{1/2}}{2\eta k_{Fdm} - 2p + (-\mu_1)^{1/2}} \right| + \ln\left| \frac{2\eta k_{Fdm} + 2p - (-\mu_1)^{1/2}}{2\eta k_{Fdm} + 2p + (-\mu_1)^{1/2}} \right| \right] \right\}$$

for $\mu_1 < 0$, (45)

$$= (4m_s/\pi a_0)(1/p^2) \sum_m \left(I_{dm} + (p^2/\eta)(1+1/\eta)\, 2(\mu_1)^{-1/2} \{ \tan^{-1}(-2p + 2\eta k_{Fdm})(\mu_1)^{-1/2} + \tan^{-1}[(2p + 2\eta k_{Fdm})(\mu_1)^{-1/2}] \} \right)$$

for $\mu_1 > 0$. (46)

Here $I_{dm} = \frac{k_{Fdm}}{\eta} - \left[\frac{k_{Fdm}^2}{4p} - \frac{p}{4\eta}\left(1+\frac{2}{\eta}\right) \right] \ln\left| \frac{2k_{Fdm}p - \eta k_{Fdm}^2 + p^2}{2k_{Fdm}p + \eta k_{Fdm}^2 - p^2} \right|$, (47)

$$\eta = (m_s/m_{dm}) - 1, \tag{48}$$

$$\mu_1 = -4p^2(1+\eta), \tag{49}$$

and a_0 is the Bohr radius. Similarly,

$$\epsilon_{sd}(\vec{p}) = \sum_m \frac{4m_{dm}}{\pi a_0 p^2} \left\{ I_{sm} + \frac{p^2}{\zeta}\left(1+\frac{1}{\zeta}\right)(-\mu_2)^{-1/2} \left[\ln\left| \frac{2\zeta k_{Fs} - 2p - (-\mu_2)^{1/2}}{2\zeta k_{Fs} - 2p + (-\mu_2)^{1/2}} \right| + \ln\left| \frac{2\zeta k_{Fs} + 2p - (-\mu_2)^{1/2}}{2\zeta k_{Fs} + 2p + (-\mu_2)^{1/2}} \right| \right] \right\}$$

for $\mu_2 < 0$, (50)

$$= \sum_m \frac{4m_{dm}}{\pi a_0 p^2} \left\{ I_{sm} + \frac{p^2}{\zeta}\left(1+\frac{1}{\zeta}\right) \frac{2}{(\mu_2)^{1/2}} \left[\tan^{-1}\left(\frac{-2p + 2\zeta k_{Fs}}{(\mu_2)^{1/2}} \right) + \tan^{-1}\left(\frac{2p + 2\zeta k_{Fs}}{(\mu_2)^{1/2}} \right) \right] \right\} \quad \text{for } \mu_2 > 0. \tag{51}$$

Here $$I_{sm} = \frac{k_{Fs}}{\zeta} - \left[\frac{k_{Fs}^2}{4p} - \frac{p}{4\zeta}\left(1+\frac{2}{\zeta}\right)\right] \times \ln\left|\frac{2k_{Fs}\,p - \zeta\,k_{Fs}^2 + p^2}{2k_{Fs}\,p + \zeta\,k_{Fs}^2 - p^2}\right| , \quad (52)$$

$$\zeta = (m_{dm}/m_s) - 1, \quad (53)$$

and $$\mu_2 = -4p^2(1+\zeta). \quad (54)$$

III. CALCULATIONS AND RESULTS

A. Model for Band Structure

The formalism developed in Sec. II is used to calculate the dielectric function of paramagnetic nickel. In the literature, there exist many calculations[13-17] for the band structure of nickel in the paramagnetic and ferromagnetic states. We have based our model on the results obtained by Hanus[13] for paramagnetic nickel using the augmented-plane-wave method. The s and d bands are admixed by the s-d interaction. The s and d characters of the wave function in a band vary as a function of $\vec{k}$. The bands have a dominantly s character at Γ_1, but d character at the X_1, L_1, and K_1 symmetry points. It demands heavy computational effort to use the results of a realistic band structure in the calculation of the dielectric matrix (1). We therefore thought it worthwhile to construct a model utilizing the calculations of Hanus, but one with noninteracting s and d bands. This model should predict the general behavior of the dielectric matrix.

We start with the energy values as a function of electron wave vector $\vec{k}$ along the principal symmetry directions [100], [110], and [111] obtained by Hanus. The noninteracting bands are obtained from the results of Hanus for the eigenvalues at the high symmetry points. The s bands are obtained by joining Γ_1 to X_4', Γ_1 to K_1, and Γ_1 to L_2' in the [010], [110], and [111] directions, respectively. For the d bands, Γ_{12} is joined to X_1 in the [010] direction; Γ_{12} and Γ_{25}' are joined with upper and lower K_1, respectively, in [110] direction; and Γ_{25}' is joined with L_1 in the [111] direction. The results of such an interpolation are presented in Fig. 1. The plots for d bands look similar to those obtained by Yamashita *et al.*[15] using the modified tight-binding approximation.

The d bands are fivefold degenerate, and the different d subbands should be assigned with different magnetic quantum numbers m. This is done by examining the d component of the basis functions[18] for the representations Γ, X, K, and L. Γ_{12} has Y_2^2 and Y_2^0 components. X_2 and X_1, which join with Γ_{12}, have both Y_2^2 and Y_2^0 components. However, K_4 has the components Y_2^2 and joins with X_2; we therefore assign $m=2$ to $\Gamma_{12}\rightarrow X_2$ and $\Gamma_{12}\rightarrow K_4$ subbands. $\Gamma_{12}\rightarrow X_1$ and $\Gamma_{12}\rightarrow K_1$ are characterized by $m=0$. L_3 has Y_2^2 and Y_2^0 components, hence the d subband $\Gamma_{12}\rightarrow L_3$ (doubly degenerate) is to be specified by $m=0$ and 2. Γ_{25}' corresponds to Y_2^{-2}, Y_2^1, and Y_2^{-1} components. X_5, which joins with Γ_{25}', has Y_2^{-2} and Y_2^1 components. However W_1' in the [120] direction and K_2 in the [110] direction, which join with X_5, have the basis functions with component Y_2^1. L_3 also joins with X_5. We therefore assign $m=1$ to the d subbands $\Gamma_{25}'\rightarrow X_5$, $\Gamma_{25}'\rightarrow K_2$, and $\Gamma_{25}'\rightarrow L_3$. The X_3 has Y_2^{-1} component, K_3 has Y_2^1 and Y_2^{-1} components, but it joins with X_3; therefore $m=-1$ is assigned to the d subbands $\Gamma_{25}'\rightarrow X_3$ and $\Gamma_{25}'\rightarrow K_3$. The $m=-1$ is also assigned to the d subband $\Gamma_{25}'\rightarrow L_3$ (doubly degenerate). The remaining subbands $\Gamma_{25}'\rightarrow K_1$ and $\Gamma_{25}'\rightarrow L_1$ are characterized by $m=-2$. The m assignments for different d subbands in the three principal symmetry directions are displayed in Table I.

It is clear from Fig. 1 that the Fermi level intersects only the s band and the d subband with $m=1$. All the other d subbands lie below the Fermi energy; hence they are completely filled. If there are z_s electrons per atom in the s band, then there will be $z_{d1}=2-z_s$ electrons per atom in the unfilled d subband with $m=1$. In the parabolic band approximation used by us

$$k_{Fs} = (3\pi^2 z_s/\Omega_0)^{1/3} \quad \text{and} \quad k_{Fd1} = (3\pi^2 z_{d1}/\Omega_0)^{1/3}.$$

Let the s band and the unfilled d subband intersect the Fermi level at the points A and B, respectively, as shown in Fig. 1, then the effective masses m_s and m_{d1} for the parabolic bands $\Gamma_1\rightarrow A$ and $\Gamma_{25}'\rightarrow B$ are given by the relations

$$m_s = \hbar^2 k_{Fs}^2 / 2[(E_F + 0.016)],$$

$$m_{d1} = \hbar^2 k_{Fd1}^2 / [2(E_F - E(\Gamma_{25}'))] .$$

Here $E(\Gamma_{25}')$ is the energy for the representation Γ_{25}' tabulated by Hanus. The energy scale has zero at Γ_1. The energy will be measured by Rydbergs and the distance will be measured in Bohr units throughout. The completely filled d subbands with two electrons per atom are filled up to zone boundary. The Brillouin zone is replaced by a sphere of radius k_B.

We still have to estimate the average effective masses associated with filled d subbands. We calculate the effective masses for bands along different symmetry directions using the eigenvalues tabulated by Hanus, but with a shift of zero, as mentioned above. Using these values of the effective masses, the eigenvalues at $k=k_B$ are calculated for all the filled d subbands and in all the three symmetry directions under consideration. We then use the Houston's method to average the eigenvalues for the three directions and to get the average eigenvalues for each of the $m=0$, 1, 2, and -2 sub-

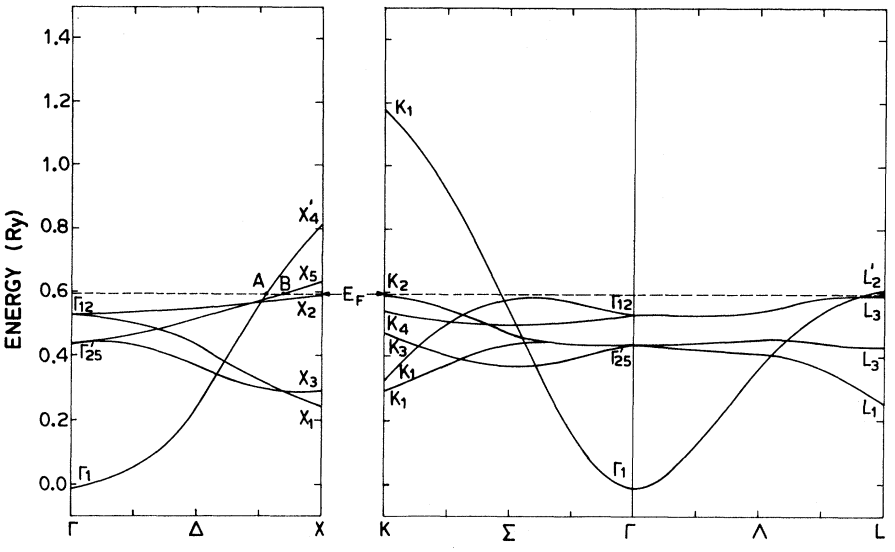

FIG. 1. Model of the noninteracting band structure for paramagnetic nickel based on the calculations of Hanus (Ref. 13).

bands. The final values of the effective masses are derived from the averaged eigenvalues.

The effective masses deduced in the manner described above are then used to calculate the model isotropic energy band structure shown in Fig. 2. The effective masses m_s, m_{d1} and the Fermi momenta k_{Fs} and k_{Fd1} are calculated for the two configurations $(3d)^9\,(4s)^1$ and $(3d)^{9.4}\,(4s)^{0.6}$. The model parabolic bands for these two configurations are shown in the Fig. 2 by the solid and dashed lines. The values of all the parameters are presented in Tables II, III, and IV.

B. 3*d* Radial Wave Function

The 3*d* radial wave function in a parametrized form (Appendix A) for the neutral atom of nickel is available from the work of Watson[19] and Clementi.[20] The 3*d* radial wave function obtained by solving the Schrödinger equation for the potential used by Hanus in his augmented-plane-wave calculations is compared in Fig. 3 with the radial wave function obtained by Watson and by Clementi. It is found that Watson's wave function is nearer to the results of our calculations. Moreover, Watson's wave function is a linear combination of four exponential functions whereas Clementi's wave function contains five terms. This simplification reduces the computational work considerably. We therefore decided to use the Watson 3*d* neutral atom radial wave function in this calculation. The parameters of the wave function are given in the Table V.

TABLE I. Assignment of the magnetic quantum number m to different d subbands along three principal symmetry directions.

[010]	[110]	[111]	m
$\Gamma_{12}\rightarrow X_2$	$\Gamma_{12}\rightarrow K_4$	$\Gamma_{12}\rightarrow L_3$	2
$\Gamma_{12}\rightarrow X_1$	$\Gamma_{12}\rightarrow K_1$	$\Gamma_{12}\rightarrow L_3$	0
$\Gamma_{25}'\rightarrow X_5$	$\Gamma_{25}'\rightarrow K_2$	$\Gamma_{25}'\rightarrow L_3$	1
$\Gamma_{25}'\rightarrow X_3$	$\Gamma_{25}'\rightarrow K_3$	$\Gamma_{25}'\rightarrow L_3$	−1
$\Gamma_{25}'\rightarrow X_3$	$\Gamma_{25}'\rightarrow K_1$	$\Gamma_{25}'\rightarrow L_1$	−2

C. Dielectric Function

In view of the model chosen for the band structure, the following types of transitions are responsible for the readjustment of electrons in response to an external field: (i) from unfilled s band to unfilled s band, (ii) from unfilled and filled d subbands to unfilled d subband, (iii) from unfilled and filled d subbands to s band, and (iv) from s band to unfilled d subband. These contributions are calculated with the help of Eqs. (11), (16), (34), and (40), respectively, for the configurations $(3d)^9\,(4s)^1$ and $(3d)^{9.4}\,(4s)^{0.6}$. The dependence on the direction of the vector $\vec{p}$ enters through the polar angles θ_p and ϕ_p in Eqs. (16), (34), and (40). Because of the choice of the polar axis and the use of spherical harmonics, the dielectric matrix does not exhibit the symmetry of the crystal.[21–23] The dielectric function $\epsilon(\vec{p})$ is calculated along the directions equivalent to the principal symmetry directions [100], [110], and [111]. For example, $\vec{p}$ is taken along all the six directions equivalent to [100], and corresponding values of $\epsilon(\vec{p})$ are obtained. For a value of $\vec{p}$, the simple average of all the six values of $\epsilon(\vec{p})$ is taken as the average $\epsilon(\vec{p})$ along [100] direction. Similarly, for [110] and [111] directions, the averaging is done over all the twelve and eight equivalent directions, respectively. The values of ϵ_{ss}, ϵ_{dd}, ϵ_{ds}, and ϵ_{sd} for the $(3d)^9\,(4s)^1$ configuration along three principal sym-

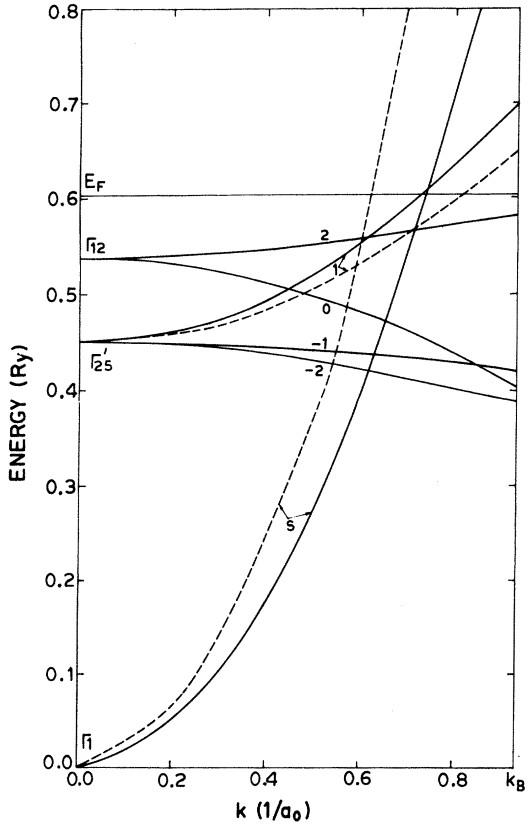

FIG. 2. Isotropic energy band structure for paramagnetic nickel. The solid lines are for the configuration $(3d)^9(4s)^1$ while dashed lines are for the configuration $(3d)^{9.4}(4s)^{0.6}$. The filled bands are identical for both the configurations. The numbers by the side of the d subbands denote the magnetic quantum number m assigned to them.

metry directions are tabulated in Table VI. Similar calculations were repeated for the configuration $(3d)^{9.4}\,(4s)^{0.6}$. The dielectric function for the configurations $(3d)^6\,(4s)^1$ and $(3d)^{9.4}\,(4s)^{0.6}$ are shown in Figs. 4 and 5, respectively. The values of ϵ_{ds} and ϵ_{sd} calculated from (45), (46) and (50), (51) are tabulated in Table VII. When we compare these free-electron approximation values with the values of ϵ_{ds} and ϵ_{sd} calculated in the manner explained above, we find that the free-electron approximation yields very high values for ϵ_{ds} and ϵ_{sd}.

TABLE II. Physical parameters for nickel.

Lattice parameter a (in units of Bohr radius a_0)	= 6.6586
Volume of the unit cell (in units of a_0^3)	=73.8034
Radius of Brillouin sphere k_B (in units of $1/a_0$)	= 0.9292

TABLE III. The Fermi radii and effective masses for s and unfilled d bands for the configurations $(3d)^9(4s)^1$ and $(3d)^{9.4}(4s)^{0.6}$. The radius is in units of $1/a_0$ and mass is in atomic units.

Configuration	$(3d)^9(4s)^1$	$(3d)^{9.4}(4s)^{0.6}$
k_{Fs}	0.7374	0.6223
k_{Fd1}	0.7374	0.8247
m_s	0.8958	0.6381
m_{d1}	3.4723	4.3431

IV. DISCUSSION

The contributions to ϵ_{dd} are separated into two parts. When $m = m'$, the transitions take place in the same subband, which should not be completely filled. In this case $m = m' = 1$. When $m \neq m'$, the transitions are from filled d subbands to the unfilled d subband. The two contributions are presented for few $\vec{p}$ vectors with components p_x, p_y, p_z in the [100], [110], and [111] directions in Table VIII. In the $m = m'$ part, it is found that $\epsilon_{dd}(\vec{p})$ decreases rapidly with increasing $\vec{p}$. The contribution of the second part, i.e., for $m \neq m'$, is very small compared to the contribution from the first part for smaller values of p while the two contributions are of the same order for larger values of p. This is because the denominator of (16) is much larger in the latter case than in the former case for small values of p while these denominators become comparable for larger values of p.

The larger value of ϵ_{dd} for the configuration $(3d)^{9.4}\,(4s)^{0.6}$ compared to the value for the configuration $(3d)^9\,(4s)^1$ results simply because of the larger number of itinerant d electrons for the former configuration. The general behavior of ϵ_{dd} for both the configurations is similar. ϵ_{ss} for the configuration $(3d)^{9.4}\,(4s)^{0.6}$ has a smaller value than that for the configuration $(3d)^9\,(4s)^1$, and this is easily explained on the basis of the larger number of s electrons available in the latter configuration.

The contributions due to interband transitions, i.e., ϵ_{ds} and ϵ_{sd}, are much smaller than ϵ_{ss} and ϵ_{dd}. For smaller values of p, ϵ_{ds} and ϵ_{sd} are of opposite sign, while for larger values of p they have the same sign. The magnitude of ϵ_{ds} and ϵ_{sd}

TABLE IV. Isotropic effective masses for different filled d subbands in atomic units.

m	0	−1	2	−2
m_{dm}	−6.5218	−29.9760	18.7257	−13.9398

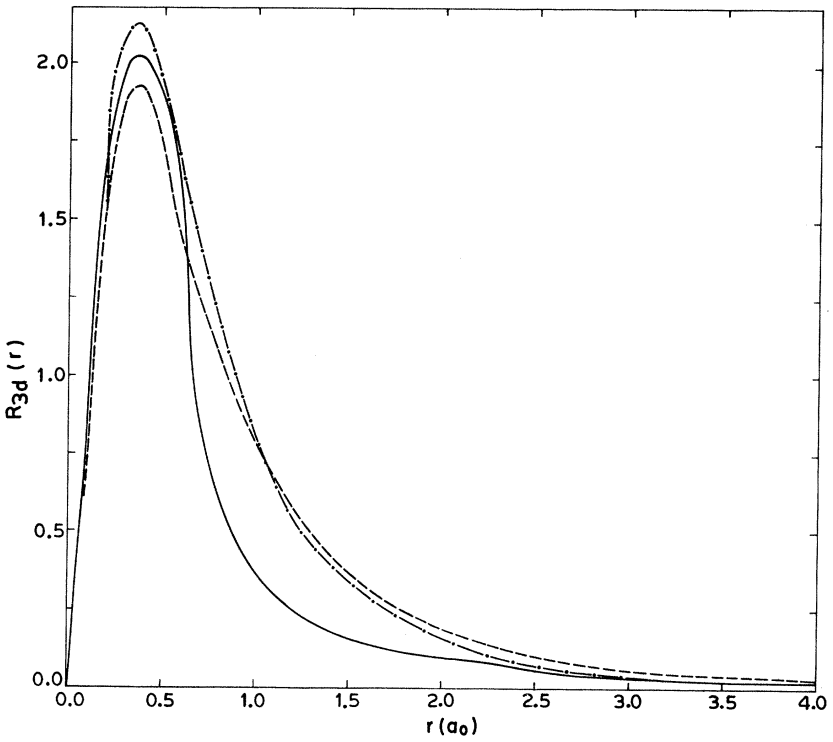

FIG. 3. Comparison of $3d$ radial wave functions of nickel. Solid curve represents the wave function obtained with the help of the Hanus potential, dashed curve represents the parametrized neutral atom wave function due to Watson (Ref. 19), while dot-dashed curve refers to Clemente's wave function (Ref. 20).

for the configuration $(3d)^{9.4}\,(4s)^{0.6}$ is smaller than the corresponding magnitude for the configuration $(3d)^{9}\,(4s)^{1}$. It is found from Table VI, that the contribution of ϵ_{dd} is largest among all contributions for $p<1.5$. But for $p>1.5$, ϵ_{dd} is of the same order of magnitude as the other contributions.

ACKNOWLEDGMENTS

The authors acknowledge the financial support from the Council of Scientific and Industrial Research, India and Department of Atomic Energy, Government of India. We wish to thank Dr. N. Singh and M. M. Pant for discussions.

APPENDIX A

We shall evaluate the integral

$$\Delta_{lm,l'm'}(\vec{p}) = \int_{N\Omega_0} \phi^*_{lm}(\vec{r}) \exp(-i\vec{p}\cdot\vec{r})\,\phi_{l'm'}(\vec{r})\,d\vec{r}\,. \tag{A1}$$

The coordinate system is shown in Fig. 6. Using

$$\phi_{lm}(\vec{r}) = R_l(r)\,Y_l^m(\theta,\phi) \tag{A2}$$

and

TABLE V. Parameters for $3d$ radial wave functions.

i	1	2	3	4
a_i	0.4475	6.5891	65.9440	99.6357
α_i	1.4397	2.7898	5.4416	9.8567

$$\exp(-i\vec{p}\cdot\vec{r}) = 4\pi \sum_{l''=0}^{\infty} (-i)^{l''} \times \sum_{m''=-l''}^{l''} Y_{l''}^{m''}(\theta_p,\phi_p)\, j_{l''}(pr)\, Y_{l''}^{m''}(\theta,\phi) \tag{A3}$$

in (A1), we get

$$\Delta_{lm,l'm'}(\vec{p}) = 4\pi \sum_{l''=0}^{\infty}(-i)^{l''} \sum_{m''=-l''}^{l''} Y_{l''}^{m''*}(\theta_p,\phi_p) \times \int_0^{\infty} j_{l''}(pr) R_l(r) R_{l'}(r) r^2\,dr \int_0^{\pi}\int_0^{2\pi} Y_{l''}^{m''}(\theta,\phi) \times Y_l^{m*}(\theta,\phi) Y_{l'}^{m'}(\theta,\phi)\,d\Omega. \tag{A4}$$

With the help of the relation

$$\int_0^{\pi}\int_0^{2\pi} Y_{l''}^{m''}(\theta,\phi) Y_l^{m*}(\theta,\phi) Y_{l'}^{m'}(\theta,\phi)\,d\Omega = \left(\frac{(2l''+1)(2l'+1)}{4\pi(2l+1)}\right)^{1/2} C(l''l'l;m''m'm) \times C(l''l'l;000),$$

we get

$$\Delta_{lm,l'm'}(\vec{p}) = 4\pi \sum_{l''=0}^{\infty} (-i)^{l''} \sum_{m''=-l''}^{l''} Y_{l''}^{m''*}(\theta_p,\phi_p) \times \int_0^{\infty} j_{l''}(pr) R_l(r) R_{l'}(r) r^2\,dr \left(\frac{(2l''+1)(2l'+1)}{4\pi(2l+1)}\right)^{1/2} \times C(l''l'l;\, m''m'm) C(l''l'l;000). \tag{A5}$$

Here the angular momentum and parity selection rules operate through the Clebsch-Gordan coefficients $C(l''l'l;\ m''m'm)$ and $C(l''l'l\,;000)$, respectively. Wigner's closed expression for C coefficients is

$$C(l''l'l;m''m'm)=\delta_{m,m''+m'}\left((2l+1)\frac{(l+l''-l')!(l-l''+l')!(l''+l'-l)!(l+m)!(l-m)!}{(l''+l'+l+1)!(l''-m'')!(l''+m'')!(l'-m')!(l'+m')!}\right)^{1/2}$$
$$\times\sum_{\nu}\frac{(-1)^{\nu+l'+m'}}{\nu!}\frac{(l'+l+m''-\nu)!(l''-m''+\nu)!}{(l-l''+l'-\nu)!(l+m-\nu)!(\nu+l''-l'-m)!}\ . \tag{A6}$$

The index ν assumes all integral values to be such that none of the factorial arguments are negative. For the $3d$ wave functions both l and l' are 2, and allowed values of l'' are 0, 2, and 4. Summing over l'' in Eq. (A5) and substituting the values of $C(l''l'l;000)$ from (A6), we get

$$\Delta_{2m,2m'}(\vec{p})=I_0\delta_{mm'}+\left(\frac{40\pi}{7}\right)^{1/2}Y_2^{m''*}(\theta_p,\phi_p)$$
$$\times C(222;m''m'm)I_2+\left(\frac{72\pi}{7}\right)^{1/2}Y_4^{m''*}(\theta_p,\phi_p)$$
$$\times C(422;m''m'm)I_4, \tag{A7}$$

where
$$I_{l''}=\int_0^\infty j_{l''}(pr)R_{3d}^2(r)r^2dr. \tag{A8}$$

We evaluate the integral $I_{l''}$ with the help of Watson's $3d$ radial wave function ,

$$R_{3d}(r)=\sum_{i=1}^{4}a_i r^2\exp(-\alpha_i r). \tag{A9}$$

The wave function involves the parameters a_i and α_i. We then get

$$I_0=\sum_{i=1}^{4}\sum_{j=1}^{4}a_i a_j A_5, \tag{A10}$$

$$I_2=\sum_{i=1}^{4}\sum_{j=1}^{4}a_i a_j(-A_5+A_4+3A_3), \tag{A11}$$

and

$$I_4=\sum_{i=1}^{4}\sum_{j=1}^{4}a_i a_j[210(A_1-A_2)-45A_3-\tfrac{10}{3}A_4+A_5], \tag{A12}$$

where

$$A_1=\frac{(\alpha_i+\alpha_j)}{p^4[p^2+(\alpha_i+\alpha_j)^2]^2}, \tag{A13}$$

$$A_2=\frac{(\alpha_i+\alpha_j)[(\alpha_i+\alpha_j)^2-3p^2]}{p^4[p^2+(\alpha_i+\alpha_j)^2]^3}, \tag{A14}$$

$$A_3=\frac{24(\alpha_i+\alpha_j)}{p^2}\left(\frac{(\alpha_i+\alpha_j)^2-p^2}{[p^2+(\alpha_i+\alpha_j)^2]^4}\right), \tag{A15}$$

$$A_4=\frac{72(\alpha_i+\alpha_j)}{p^2}\left(\frac{-5p^4-(\alpha_i+\alpha_j)^4+10p^2(\alpha_i+\alpha_j)^2}{[p^2+(\alpha_i+\alpha_j)^2]^5}\right), \tag{A16}$$

and

$$A_5=240(\alpha_i+\alpha_j)\left(\frac{3p^4+3(\alpha_i+\alpha_j)^4-10p^2(\alpha_i+\alpha_j)^2}{[p^2+(\alpha_i+\alpha_j)^2]^6}\right). \tag{A17}$$

We give below the specific values of $\Delta_{lm,lm'}$ which have been used in our calculations:

$$\Delta_{20,21}(\vec{p})=\tfrac{2}{7}(5\pi)^{1/2}Y_2^{-1*}I_2-\tfrac{2}{7}(30\pi)^{1/2}Y_4^{-1*}I_4,$$
$$\Delta_{21,21}(\vec{p})=I_0-\tfrac{2}{7}(5\pi)^{1/2}Y_2^{0*}I_2-\tfrac{8}{7}(\pi)^{1/2}Y_4^{0*}I_4,$$
$$\Delta_{2-1,21}(\vec{p})=\tfrac{2}{7}(30\pi)^{1/2}Y_2^{-2*}I_2-\tfrac{4}{7}(10\pi)^{1/2}Y_4^{-2*}I_4, \tag{A18}$$
$$\Delta_{22,21}(\vec{p})=-\tfrac{2}{7}(30\pi)^{1/2}Y_2^{1*}I_2-\tfrac{2}{7}(5\pi)^{1/2}Y_4^{1*}I_4,$$
$$\Delta_{2-2,21}(\vec{p})=-2(5\pi/7)^{1/2}Y_4^{-3*}I_4.$$

TABLE VI. Relative Magnitudes of ϵ_{ss}, ϵ_{dd}, ϵ_{ds}, and ϵ_{sd} for the configuration $(3d)^9(4s)^1$. Here $\vec{p}$ is measured in units of $1/a_0$.

$\lvert\vec{p}\rvert$	$-\epsilon_{ss}(\vec{p})$	$-\epsilon_{dd}(\vec{p})$	$-\epsilon_{ds}(\vec{p})$	$-\epsilon_{sd}(\vec{p})$
		[100] direction		
0.2	20.8969	79.0620	4.2028	−1.1100
0.4	5.1257	18.0548	1.1078	−0.6207
0.6	2.2028	6.9253	0.4552	−0.4699
0.8	1.1765	3.1834	0.1962	0.2185
1.0	0.6971	1.5736	0.0922	0.0082
1.5	0.1718	0.2289	0.0162	0.0059
2.0	0.0437	0.0359	0.0049	0.0010
2.5	0.0169	0.0096	0.0020	0.0001
3.0	0.0079	0.0035	0.0010	0.0000
3.5	0.0042	0.0016	0.0005	0.0000
4.0	0.0024	0.0008	0.0003	0.0000
4.5	0.0015	0.0005	0.0002	0.0000
		[110] direction		
0.2828	10.3838	38.3628	2.3787	−0.8518
0.5657	2.4955	8.0700	0.5469	−0.3043
0.8485	1.0293	2.7263	0.1825	−0.0751
1.1314	0.5072	1.0549	0.0619	0.0064
1.4142	0.2444	0.3882	0.0232	0.0656
2.1213	0.0339	0.0313	0.0043	0.0023
2.8284	0.0101	0.0062	0.0013	0.0002
3.5355	0.0041	0.0018	0.0006	0.0000
4.2426	0.0019	0.0007	0.0003	0.0000
		[111] direction		
0.3464	6.8787	24.8435	1.6021	5.3939
0.6928	1.6171	6.8287	0.3457	3.2891
1.0392	0.6332	1.4466	0.0933	0.0482
1.3856	0.2665	0.4458	0.0261	0.0116
1.7321	0.0831	0.1065	0.0103	0.0087
2.5981	0.0144	0.0103	0.0019	0.0006
3.4641	0.0044	0.0020	0.0006	0.0001
4.3301	0.0018	0.0005	0.0003	0.0000

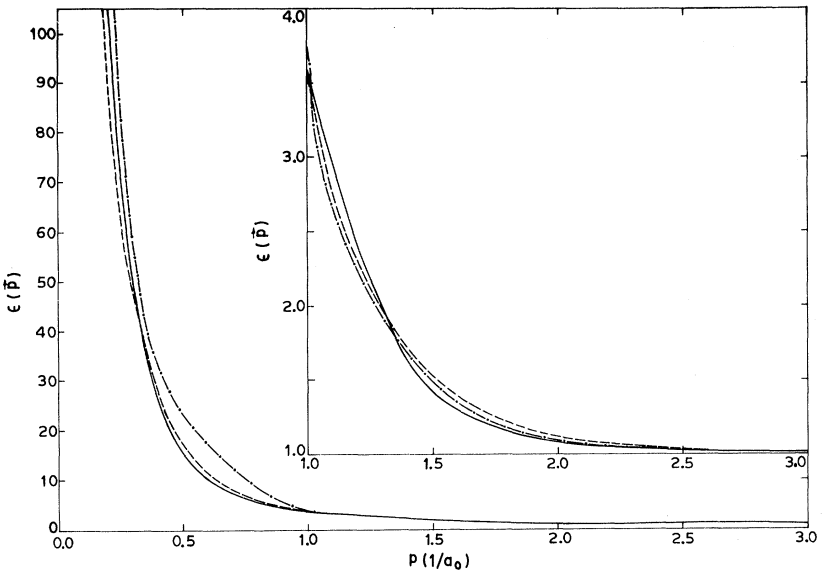

FIG. 4. $\epsilon(\tilde{p})$ versus $\tilde{p}$ for the configuration $(3d)^9(4s)^1$. $\epsilon(\tilde{p})$ is represented by solid, dashed, and dot-dashed lines along [100], [110], and [111] directions, respectively. In the upper-right-hand corner, $\epsilon(\tilde{p})$ is plotted on a magnified scale for $p > 1$.

Here the arguments of the spherical harmonics are θ_p and ϕ_p .

APPENDIX B

In this Appendix, we shall evaluate the angular integral

$$I = \int_0^{\pi}\int_0^{2\pi} \frac{Y_2^{m*}(\theta_k,\phi_k)\, Y_2^{m}(\theta_k,\phi_k)}{a - b\cos\theta_{kp}}\, d\Omega_k \,. \qquad \text{(B1)}$$

We rotate the coordinate system shown in Fig. 6 through an angle ϕ_p about the Z axis and then through an angle θ_p about the new Y' axes. The new Z'' axis obtained after the second rotation coincides with vector $\tilde{p}$. If α, β, γ are the Euler angles which rotate the coordinate system X, Y, Z to the coordinate system X'', Y'', Z'', then $\alpha = \phi_p$, $\beta = \theta_p$, and $\gamma = 0$. The spherical harmonics in the old coordinate system X, Y, Z are transformed into the spherical harmonics in new coordinate system X'', Y'', Z'' with the help of rotation matrices $D(\alpha, \beta, \gamma)$, i.e.,

$$Y_l^{m'}(\theta,\phi) = \sum_m D^l_{m,m'}(\alpha\ \beta\ \gamma) Y_l^m(\theta_k,\phi_k) \,. \qquad \text{(B2)}$$

Here θ, ϕ are the polar angles of vector $\tilde{k}$ in the

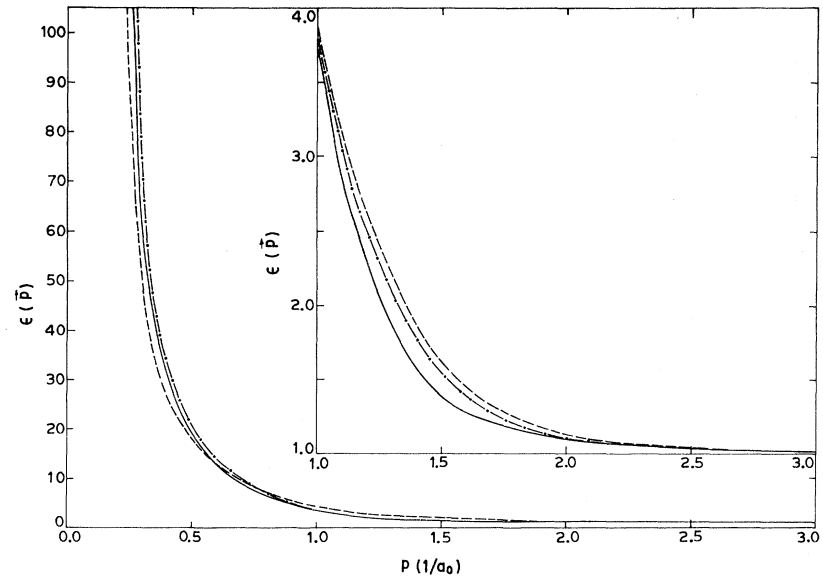

FIG. 5. $\epsilon(\tilde{p})$ versus $\tilde{p}$ for the configuration $(3d)^{9.4}\ (4s)^{0.6}$. The description is the same as for Fig. 4.

TABLE VII. $\epsilon_{ds}(\vec{p})$ and $\epsilon_{sd}(\vec{p})$ using the free-electron approximation for the configuration $(3d)^9(4s)^1$. p is measured in units of $1/a_0$.

$\lvert\vec{p}\rvert$	$-\epsilon_{ds}(\vec{p})$	$-\epsilon_{sd}(\vec{p})$
0.2	240.6554	−54.5128
0.4	49.2092	−11.8872
0.6	17.7336	− 3.7036
0.8	7.3659	− 1.3607
1.0	3.3308	0.3689
1.5	0.5849	0.2838
2.0	0.1787	0.1390
2.5	0.0721	0.0412
3.0	0.0345	0.0176
3.5	0.0186	0.0089

new coordinate system X'', Y'', Z'' while θ_k, ϕ_k are zenith and azimuthal angles in the old coordinate system X, Y, Z. The angle θ_{kp} becomes θ in the new coordinate system. Multiplying both sides by $D^{*l}_{m''m'}(\alpha\ \beta\ \gamma)$, summing over m', and using the orthogonality property of rotation matrices, we get

$$\sum_{m'} D^{l*}_{m''m'}(\alpha\beta\gamma)\, Y_l^{m'}(\theta,\phi) = Y_l^{m''}(\theta_k,\phi_k). \quad \text{(B3)}$$

Replacing m'' by m and using the property

TABLE VIII. The values of $\epsilon_{dd}(\vec{p})$ for $m=m'=1$ and for $m\neq m'$, for the configuration $(3d)^9(4s)^1$. p is measured in units of $1/a_0$.

p_x	p_y	p_z	$-\epsilon_{dd}(\vec{p})$ $m=m'$ $m=1$	$-\epsilon_{dd}(\vec{p})$ $m\neq m'$
0.2	0	0	79.3344	0.0089
0.4	0	0	18.2886	0.0283
0.6	0	0	7.1106	0.0459
0.8	0	0	3.3220	0.0528
1.0	0	0	1.6729	0.0484
1.5	0	0	0.2496	0.0271
2.0	0	0	0.0349	0.0139
2.5	0	0	0.0069	0.0072
3.0	0	0	0.0016	0.0037
3.5	0	0	0.0004	0.0019
0.2	0.2	0	38.6063	0.0164
0.4	0.4	0	8.2154	0.0435
0.6	0.6	0	2.8005	0.0526
0.8	0.8	0	1.0793	0.0426
1.0	1.0	0	0.3900	0.0303
1.5	1.5	0	0.0232	0.0119
2.0	2.0	0	0.0026	0.0047
2.5	2.5	0	0.0003	0.0019
0.2	0.2	0.2	24.8017	0.0418
0.4	0.4	0.4	4.7603	0.0664
0.6	0.6	0.6	1.3849	0.0618
0.8	0.8	0.8	0.4091	0.0367
1.0	1.0	1.0	0.0869	0.0195
1.5	1.5	1.5	0.0055	0.0048
2.0	2.0	2.0	0.0006	0.0014

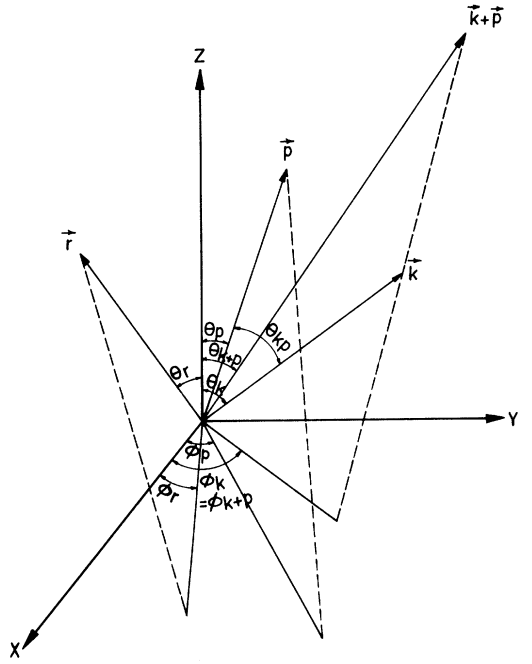

FIG. 6. Coordinate system.

$$D^{l*}_{mm'}(\alpha\beta\gamma) = D^{l}_{m'm}(-\gamma,-\beta,-\alpha),$$

we obtain

$$Y_l^m(\theta_k,\phi_k) = \sum_{m'} D^l_{m'm}(-\gamma,-\beta,-\alpha)\, Y_l^{m'}(\theta,\phi). \quad \text{(B4)}$$

For the sake of convenience, the arguments $(-\gamma, -\beta, -\alpha)$ of $D^l_{m'm}$ are dropped. Using the relation $Y_2^{m*}(\theta_k,\phi_k) = (-1)^m Y_2^{-m}(\theta_k,\phi_k)$ and (B4) in (B1), we can write

$$I = (-1)^m \sum_{m'}\sum_{m''} D^2_{m'm} D^2_{m''m} \times \int_0^{\pi}\int_0^{2\pi} \frac{Y_2^{m'}(\theta,\phi) Y_2^{m''}(\theta,\phi)}{a - b\cos\theta}\, d\Omega \quad \text{(B5)}$$

$$= (-1)^m 2\pi \sum_{m'} D^2_{m'm} D^2_{-m'-m} \times \int_0^{\pi} \frac{P_2^{m'}(\cos\theta) P_2^{-m'}(\cos\theta)\sin\theta\, d\theta}{a - b\cos\theta}. \quad \text{(B6)}$$

For $l=2$, the allowed values of m' in the sum are $0, \pm1, \pm2$. Therefore,

$$I = (-1)^m [D^2_{0m} D^2_{0-m} I_0 + (D^2_{1m} D^2_{-1-m} + D^2_{-1m} D^2_{1-m}) I_1 + (D^2_{2m} D^2_{-2-m} + D^2_{-2m} D^2_{2-m}) I_2], \quad \text{(B7)}$$

where

$$I_{m'} = 2\pi \int_0^{\pi} \frac{P_2^{m'}(\cos\theta) P_2^{-m'}(\cos\theta)}{a - b\cos\theta} \sin\theta\, d\theta. \quad \text{(B8)}$$

The elements of rotation matrices are evaluated with the help of the general expression

$$D^{l}_{m',m}(\alpha\beta\gamma) = \exp(-im'\alpha)\exp(-im\gamma)\sum_s (-1)^s \times \frac{[(l+m)!(l-m)!(l+m')!(l-m')!]^{1/2}}{s!(l-s-m')!(l+m-s)!(m'+s-m)!} \times (\cos\tfrac{1}{2}\beta)^{2l+m-m'-2s}(-\sin\tfrac{1}{2}\beta)^{m'-m+2s}. \quad \text{(B9)}$$

Here the sum is over integer values of s for which the factorial arguments are greater than or equal to zero. The matrix elements of rotation matrix $D^{l}_{m',m}(-\gamma,-\beta,-\alpha)$ can be written easily for $l=2$ with the help of (B9). The coefficients of I_0, I_1, and I_2 in (B7) are given by the following expressions:

$$D^2_{01}D^2_{0-1} = -\tfrac{3}{2}\sin^2\beta\cos^2\beta,$$

$$D^2_{11}D^2_{-1-1} + D^2_{-11}D^2_{1-1} = \tfrac{1}{2}(4\cos^2\beta - 3\cos^2\beta + 1), \quad \text{(B10)}$$

$$\text{and} \quad D^2_{21}D^2_{-2-1} + D^2_{-21}D^2_{2-1} = -\tfrac{1}{2}\sin^2\beta(\cos^2\beta + 1).$$

APPENDIX C

To evaluate the integral

$$I = \int_0^{\pi}\int_0^{2\pi} \frac{[F_2(|\vec{k}+\vec{p}|)]^2 Y_2^m(\theta_{k+p},\phi_{k+p}) Y_2^{m*}(\theta_{k+p},\phi_{k+p})\, d\Omega_k}{a' - b\cos\theta_{kp}}, \quad \text{(C1)}$$

we proceed in a manner similar to that described in Appendix B. We get finally

$$I = (-1)^m [D^2_{0m}D^2_{0-m}I_0' + (D^2_{-1m}D^2_{1-m} + D^2_{1m}D^2_{-1-m})I_1' + (D^2_{-2m}D^2_{2-m} + D^2_{2m}D^2_{-2-m})I_2']. \quad \text{(C2)}$$

Here $$I'_{m'} = 2\pi\int_0^{\pi} \frac{[F_2(|\vec{k}+\vec{p}|)]^2 P_2^m(\cos\theta'_{k+p}) P_2^{-m}(\cos\theta'_{k+p})\sin\theta\, d\theta}{a' - b\cos\theta}. \quad \text{(C3)}$$

θ'_{k+p} and ϕ'_{k+p} are the polar angles of vector $\vec{k}+\vec{p}$ in the coordinate system X'', Y'', Z''. It can be seen from the Fig. 6 that

$$\phi'_{k+p} = \phi$$

and $$\cos\theta'_{k+p} = \vec{p}\cdot(\vec{k}+\vec{p})/|\vec{p}||\vec{k}+\vec{p}|$$

$$= (p + k\cos\theta)(k^2 + p^2 + 2kp\cos\theta)^{-1/2}. \quad \text{(C4)}$$

Using (C4) in (C3), the principal value of the integral $I'_{m'}$ can be evaluated.

[1] J. Lindhard, Kgl. Danske Videnskab. Selskab, Mat.-Fys. Medd. 28, No. 8 (1954).

[2] P. Nozières and D. Pines, Phys. Rev. 109, 741 (1958); 109, 762 (1958); 109, 1062 (1958); 111, 442 (1958); 113, 1254 (1959).

[3] H. Ehrenreich and M. H. Cohen, Phys. Rev. 115, 786 (1959).

[4] S. L. Adler, Phys. Rev. 126, 413 (1962).

[5] D. R. Penn, Phys. Rev. 128, 2093 (1962).

[6] H. Nara, J. Phys. Soc. Japan 20, 778 (1965); 20, 1097 (1965).

[7] G. Srinivasan, Phys. Rev. 178, 1244 (1969).

[8] E. Hayashi and M. Shimizu, J. Phys. Soc. Japan 26, 1396 (1969); 27, 43 (1969).

[9] L. J. Sham and J. H. Ziman, in *Solid State Physics*, edited by F. Seitz and D. Turnbull (Academic, New York, 1963), Vol. 15, p. 221.

[10] N. Wiser, Phys. Rev. 129, 62 (1963).

[11] I. S. Gradshteyn and I. M. Ryzhik, in *Table of Integrals, Series, and Products* (Academic, New York, 1965), p. 60.

[12] M. E. Rose, *Elementry Theory of Angular Momentum* (Wiley, New York, 1957), p. 48.

[13] J. G. Hapus, MIT Solid State and Molecular Theory Group, Quarterly Progress Report No. 44, 1962 (unpublished), p. 29.

[14] L. F. Mattheiss, Phys. Rev. 134, A970 (1964).

[15] J. Yamashita, M. Fukuchi, and S. Wakoh, J. Phys. Soc. Japan 18, 999 (1963); 19, 1342 (1964); S. Wakoh, *ibid.* 20, 1894 (1965).

[16] L. Hodges, H. Ehrenreich, and N. D. Lang, Phys. Rev. 152, 505 (1966); H. Ehrenreich and L. Hodges, in *Methods in Computational Physics* (Academic, New York, 1968), Vol. 8, p. 149.

[17] J. W. D. Connolly, Phys. Rev. 159, 415 (1967).

[18] J. Callaway, *Energy Band Theory* (Academic, New York, 1964).

[19] R. E. Watson, MIT Solid State and Molecular Theory Group, Technical Report No. 12, 1952 (unpublished).

[20] E. Clementi, in *Tables of Atomic Functions* (IBM Corporation, San Jose, Calif., 1965).

[21] J. L. Fry, Phys. Rev. 179, 892 (1969).

[22] J. V. Koppel, Ph. D. thesis, University of California, San Diego, Calif., 1968 (unpublished).

[23] L. Liu and D. Brust, Phys. Rev. 173, 777 (1968).